An efficient solution of Liouville-von Neumann equation that is applicable to zero and finite temperatures

Heng Tian, and GuanHua Chen

Citation: The Journal of Chemical Physics **137**, 204114 (2012);
View online: https://doi.org/10.1063/1.4767460
View Table of Contents: http://aip.scitation.org/toc/jcp/137/20
Published by the American Institute of Physics

Articles you may be interested in

Time-dependent quantum transport: An efficient method based on Liouville-von-Neumann equation for single-electron density matrix
The Journal of Chemical Physics **137**, 044113 (2012); 10.1063/1.4737864

Time-dependent density functional theory for quantum transport
The Journal of Chemical Physics **133**, 114101 (2010); 10.1063/1.3475566

Exact dynamics of dissipative electronic systems and quantum transport: Hierarchical equations of motion approach
The Journal of Chemical Physics **128**, 234703 (2008); 10.1063/1.2938087

Padé spectrum decompositions of quantum distribution functions and optimal hierarchical equations of motion construction for quantum open systems
The Journal of Chemical Physics **134**, 244106 (2011); 10.1063/1.3602466

A hybrid stochastic hierarchy equations of motion approach to treat the low temperature dynamics of non-Markovian open quantum systems
The Journal of Chemical Physics **139**, 134106 (2013); 10.1063/1.4822043

Dissipative time-dependent quantum transport theory
The Journal of Chemical Physics **138**, 164121 (2013); 10.1063/1.4802592

An efficient solution of Liouville-von Neumann equation that is applicable to zero and finite temperatures

Heng Tian[1,a)] and GuanHua Chen[1,2,3,b)]
[1]*Department of Chemistry, The University of Hong Kong, Hong Kong*
[2]*Department of Physics, The University of Hong Kong, Hong Kong*
[3]*Centre for Theoretical and Computational Physics, The University of Hong Kong, Hong Kong*

(Received 23 August 2012; accepted 31 October 2012; published online 27 November 2012)

Application of quantum dissipation theory to electronic dynamics has been limited to model systems with few energy levels, and its numerical solutions are mostly restricted to high temperatures. A highly accurate and efficient numerical algorithm, which is based on the Chebyshev spectral method, is developed to integrate a single-particle Liouville-von Neumann equation, and the two long-standing limitations of quantum dissipation theory are resolved in the context of quantum transport. Its computational time scales to $\mathcal{O}(N^3)$ with N being the number of orbitals involved, which leads to a reality for the quantum mechanical simulation of real open systems containing hundreds or thousands of atomic orbitals. More importantly, the algorithm spans both finite and zero temperatures. Numerical calculations are carried out to simulate the transient current through a metallic wire containing up to 1000 orbitals. © *2012 American Institute of Physics*. [http://dx.doi.org/10.1063/1.4767460]

I. INTRODUCTION

Quantum dissipation theory deals with the dynamics of open systems. Master equation or Liouville-von Neumann equation is normally used to simulate the open systems by following the time evolution of the corresponding reduced density matrix of the system. As the reduced density matrix of a system is a product of two many-body wave functions, the solution of the Liouville-von Neumann equation is time-consuming as the computational time scales factorially with the number of orbitals involved. As a result, the study of open systems is limited to the model systems containing few levels. Another long-standing problem is that the conventional numerical methods in quantum dissipation theory are applicable to either zero or finite temperature. No existing method spans zero to high temperatures.

On the other hand, quantum chemistry methods including first-principles methods have been highly successful in calculating electronic structures containing hundreds or thousands of orbitals. It may be constructive to combine both fields, quantum dissipation theory and quantum chemistry, by extending the realm of quantum chemistry to open systems, or applying the numerical techniques developed for quantum chemistry to quantum dissipation theory. Efforts along this direction have been made, e.g., based on the holographic electron density theorem, a time-dependent density-functional theory for open system was proposed.[1] In this article, we represent a highly efficient numerical algorithm for a Liouville-von Neumann equation, which is based on the Chebyshev spectral method,[2] a technique commonly adopted in the field of quantum chemistry amongst many others. The computational time of the resulting method scales $\mathcal{O}(N^3)$, with N being the number of orbitals involved. Simulation of realistic open electronic systems is thus a reality. Moreover, the method spans from zero to finite temperatures, solving yet another long-standing challenge in quantum dissipation theory.

II. THEORY AND NUMERICAL FRAMEWORK

Our objective is to develop the first-principles quantum dissipation theory by combining the Liouville-von Neumann equation and density-functional theory. As density-functional theory (DFT)[3] or time-dependent density-functional theory (TDDFT)[4] is in essence an effective single-electron theory, it is suffice to consider the effective single-electron model such as Kohn-Sham (KS) Hamiltonian

$$\mathbf{H}_{\mathrm{T}} = \mathbf{H}_{\mathrm{C}} + \sum_{\alpha}(\mathbf{H}_{\alpha} + \mathbf{H}_{\alpha\mathrm{C}}), \tag{1}$$

where, $\mathbf{H}_{\mathrm{C}}$ denotes the Hamiltonian for the device part, $\mathbf{H}_{\alpha}$ for the electrode ($\alpha = \mathrm{L,R}$), and $\mathbf{H}_{\alpha\mathrm{C}}$ for the tunneling between the device part and the electrode. In the language of second quantization, they can be succinctly expressed as follows:

$$\mathbf{H}_{\mathrm{C}} = \sum_{\mu\nu} \boldsymbol{h}_{\mu\nu} a_{\mu}^{\dagger} a_{\nu}, \mathbf{H}_{\alpha} = \sum_{k\in\alpha} \epsilon_{\alpha k}\, d_{\alpha k}^{\dagger} d_{\alpha k}, \tag{2}$$

$$\mathbf{H}_{\alpha\mathrm{C}} = \sum_{\mu}\sum_{k\in\alpha} \boldsymbol{t}_{\alpha k\mu} d_{\alpha k}^{\dagger} a_{\mu} + \mathrm{H.C.}, \tag{3}$$

of which, $a_{\mu}^{\dagger}(a_{\nu})$ creates(annihilates) an electron in the corresponding orthonormal basis $|\phi_{\mu}\rangle(|\phi_{\nu}\rangle)$ of the device part, and $d_{\alpha k}^{\dagger}(d_{\alpha k})$ creates(annihilates) an electron in the eigenstate $|k_{\alpha}\rangle$ of the electrode α. And accordingly, $\boldsymbol{h}_{\mu\nu} = \langle\mu|\hat{h}(\boldsymbol{r}, t)|\nu\rangle$, $\epsilon_{\alpha k} = \langle k_{\alpha}|\hat{h}(\boldsymbol{r}, t)|k_{\alpha}\rangle$, and $\boldsymbol{t}_{\alpha k\mu} = \langle k_{\alpha}|\hat{h}(\boldsymbol{r}, t_0)|\mu\rangle$. Note that for DFT or TDDFT, $\hat{h}$ is the KS Fock operator.

It is more convenient to work in the reservoir $\mathbf{H}_{\mathrm{B}}$-interaction picture,[5] where $\mathbf{H}_{\mathrm{B}} = \sum_{\alpha}\mathbf{H}_{\alpha}$. Hereinafter, any operator in this picture is denoted with *tilde* on its top.

a)Electronic mail: tianheng@yangtze.hku.hk.
b)Electronic mail: ghc@yangtze.hku.hk.

 © 2012 American Institute of Physics

After transformation into this interaction picture, the Hamiltonian $\mathbf{H}_{\rm T}$ becomes

$$\tilde{\mathbf{H}}_{\rm T}(t) = \mathbf{H}_{\rm C} + \sum_{\alpha} \tilde{\mathbf{H}}_{\alpha{\rm C}}(t), \tag{4}$$

where

$$\tilde{\mathbf{H}}_{\alpha{\rm C}}(t) = \sum_{\mu} \left[\tilde{b}^{\dagger}_{\alpha\mu}(t) a_{\mu} + a^{\dagger}_{\mu} \tilde{b}_{\alpha\mu}(t)\right],$$

$$\tilde{b}^{\dagger}_{\alpha\mu}(t) = \sum_{k} \boldsymbol{t}_{\alpha k\mu} \tilde{d}^{\dagger}_{\alpha k}(t) = \sum_{k} \boldsymbol{t}_{\alpha k\mu} {\rm e}^{i\int_{t_0}^{t}[\epsilon_{\alpha k}+\Delta_{\alpha}(\tau)]{\rm d}\tau} d^{\dagger}_{\alpha k},$$

in which $\Delta_{\alpha}(t)$ is the rigid uniform shift for all single-electron levels in electrode α under the time-dependent voltage on this electrode.[6]

Since $\mathbf{H}_{\alpha}$ is bounded both from below and above, in this article, the whole discussion is restricted to the case where the spectral $\epsilon_{\alpha k}$'s are the same for different α and at least piece-wisely continuously distributed in a finite interval $[\omega_{min}, \omega_{max}] = [\bar{\omega} - \Omega, \bar{\omega} + \Omega]$, where $\bar{\omega} = (\omega_{max} + \omega_{min})/2$, $\Omega = (\omega_{max} - \omega_{min})/2$.

Thus, we have

$$\tilde{\mathbf{H}}_{\alpha{\rm C}}(t) = \sum_{\mu} \Omega \int_{-1}^{1} {\rm d}x \left[{\rm e}^{i\Omega x(t-t_0)} \tilde{b}^{\dagger}_{\alpha\mu}(x,t) a_{\mu} + {\rm H.C.},\right.$$

where

$$\tilde{b}^{\dagger}_{\alpha\mu}(x,t) = \sum_{k\in\alpha} \delta(\Omega x + \bar{\omega} - \epsilon_{\alpha k})\, \boldsymbol{t}_{\alpha k\mu}\, d^{\dagger}_{\alpha k}\, {\rm e}^{i\int_{t_0}^{t} {\rm d}\tau(\Delta_{\alpha}(\tau)+\bar{\omega})}.$$

After some algebraic manipulations, we can obtain the following hierarchical equations of motion (HEOM) in which the first one is the foremost Liouville-von Neumann equation:[5,7–10]

$$i\dot{\boldsymbol{\sigma}}_{\mu\nu}(t) = -\sum_{\alpha} \Omega \int_{-1}^{1} {\rm d}x \left[{\rm e}^{i\Omega x(t-t_0)} \boldsymbol{\varphi}_{\alpha,\mu\nu}(x,t) - {\rm H.C.}\right] + [\boldsymbol{h}(t), \boldsymbol{\sigma}(t)]_{\mu\nu}, \tag{5}$$

$$\begin{aligned} i\dot{\boldsymbol{\varphi}}_{\alpha,\mu\nu}(x,t) = &-[\Delta_{\alpha}(t) + \bar{\omega}]\boldsymbol{\varphi}_{\alpha,\mu\nu}(x,t) + \sum_{\mu'} \boldsymbol{h}_{\mu\mu'} \boldsymbol{\varphi}_{\alpha,\mu'\nu}(x,t) \\ &- \sum_{\mu'} \boldsymbol{\sigma}_{\mu\mu'}(t) \boldsymbol{\Lambda}_{\alpha,\mu'\nu}(x,t) + \bar{f}_{\alpha}(x) \boldsymbol{\Lambda}_{\alpha,\mu\nu}(x,t) \\ &+ \Omega \sum_{\alpha'} \int_{-1}^{1} {\rm d}x'\, {\rm e}^{-i\Omega x'(t-t_0)} \boldsymbol{\psi}_{\alpha'\alpha,\mu\nu}(x',x,t), \end{aligned} \tag{6}$$

$$\begin{aligned} i\dot{\boldsymbol{\psi}}_{\alpha'\alpha,\mu\nu}(x',x,t) = &[\Delta_{\alpha'}(t) - \Delta_{\alpha}(t)]\boldsymbol{\psi}_{\alpha'\alpha,\mu\nu}(x',x,t) \\ &+ \sum_{\mu'} \boldsymbol{\Lambda}^{*}_{\alpha',\mu\mu'}(x',t) \boldsymbol{\varphi}_{\alpha,\mu'\nu}(x,t) \\ &- \sum_{\mu'} \boldsymbol{\varphi}^{\dagger}_{\alpha',\mu\mu'}(x',t) \boldsymbol{\Lambda}_{\alpha,\mu'\nu}(x,t). \end{aligned} \tag{7}$$

Here, $\bar{f}_{\alpha}(x) = f_{\alpha}(\Omega x + \bar{\omega})$ is the Fermi distribution function for the electrode α being *always at equilibrium*,

$$\boldsymbol{\sigma}_{\mu\nu}(t) \equiv {\rm tr}_{\rm T}\left[a^{\dagger}_{\nu} a_{\mu} \tilde{\boldsymbol{\rho}}_{\rm T}(t)\right], \tag{8}$$

$$\boldsymbol{\varphi}_{\alpha,\mu\nu}(x,t) \equiv {\rm tr}_{\rm T}\left[\tilde{b}^{\dagger}_{\alpha\nu}(x,t)\, a_{\mu}\, \tilde{\boldsymbol{\rho}}_{\rm T}(t)\right], \tag{9}$$

$$\boldsymbol{\psi}_{\alpha'\alpha,\mu\nu}(x',x,t) = {\rm tr}_{\rm T}\left\{\tilde{b}^{\dagger}_{\alpha\nu}(x,t)\, \tilde{b}_{\alpha'\mu}(x',t)[\tilde{\boldsymbol{\rho}}_{\rm T}(t) - \tilde{\boldsymbol{\rho}}_{\rm T}(-\infty)]\right\}, \tag{10}$$

$$\begin{aligned} \boldsymbol{\Lambda}_{\alpha,\mu\nu}(x,t) &= \sum_{k\in\alpha} \delta(\Omega x + \bar{\omega} - \epsilon_{\alpha k}) \boldsymbol{t}^{*}_{\alpha k\mu} \boldsymbol{t}_{\alpha k\nu} {\rm e}^{-i\Omega x(t-t_0)} \\ &= \boldsymbol{\Lambda}_{\alpha,\mu\nu}(x) {\rm e}^{-i\Omega x(t-t_0)}, \end{aligned} \tag{11}$$

are the reduced single-particle density matrix (RSDM), frequency-dispersed first- and second-tier auxiliary RSDM, and the time-dependent line-width matrix, respectively, where $\tilde{\boldsymbol{\rho}}_{\rm T}(-\infty)$ corresponds to an extreme situation where there is no tunneling between the device and the electrode. The transient current,

$$I_{\alpha}(t) = i\Omega {\rm tr}_{\rm T}\left[\int_{-1}^{1} {\rm d}x\, {\rm e}^{-i\Omega x(t-t_0)} \boldsymbol{\varphi}_{\alpha}(x,t) - {\rm H.C.}\right], \tag{12}$$

which is of primary concern in time-dependent quantum transport, can be obtained from this HEOM.

To integrate Eqs. (5)–(7), we propose the Chebyshev spectral decomposition[2] scheme by making use of the Jacobi-Anger identity,[11]

$${\rm e}^{-i\Omega x(t-t_0)} = J_0(\Omega(t-t_0)) + \sum_{n=1}^{\infty} 2(-i)^n J_n(\Omega(t-t_0)) T_n(x), \tag{13}$$

where J_n is the Bessel function of the first kind of the integer order and T_n is the Chebyshev polynomial of the first kind. Substituting Eq. (13) into the right hand side of Eqs. (5) and (6), we re-discretize Eqs. (5)–(7) and reduce them into the following set of coupled ordinary differential equations:

$$\begin{aligned} i\dot{\boldsymbol{\sigma}}(t) = &-\sum_{\alpha} \sum_{k=0}^{\infty} [\Omega i^k J_k(\Omega(t-t_0)) \boldsymbol{\varphi}_{\alpha,k}(t) - {\rm H.C.}] \\ &+ [\boldsymbol{h}(t), \boldsymbol{\sigma}(t)], \end{aligned} \tag{14}$$

$$\begin{aligned} i\dot{\boldsymbol{\varphi}}_{\alpha,k}(t) = &\sum_{\alpha'} \sum_{k'=0}^{\infty} (-i)^{k'} \Omega J_{k'}(\Omega(t-t_0)) \boldsymbol{\psi}_{\alpha'k',\alpha k}(t) \\ &+ [\boldsymbol{h}(t) - \bar{\omega} - \Delta_{\alpha}(t)]\boldsymbol{\varphi}_{\alpha,k}(t) \\ &+ (2-\delta_{k,0})[\boldsymbol{\Xi}_{\alpha,k}(t) - \boldsymbol{\sigma}(t)\boldsymbol{\Pi}_{\alpha,k}(t)], \end{aligned} \tag{15}$$

$$\begin{aligned} i\dot{\boldsymbol{\psi}}_{\alpha'k',\alpha k}(t) = &(2-\delta_{k'0})\boldsymbol{\Pi}^{*}_{\alpha',k'}(t)\boldsymbol{\varphi}_{\alpha,k}(t) \\ &- (2-\delta_{k0})\boldsymbol{\varphi}^{\dagger}_{\alpha',k'}(t)\boldsymbol{\Pi}_{\alpha,k}(t) \\ &+ [\Delta_{\alpha'}(t) - \Delta_{\alpha}(t)]\boldsymbol{\psi}_{\alpha'k',\alpha k}(t), \end{aligned} \tag{16}$$

where the discretized first- and second-tier auxiliary RSDM are defined

$$\boldsymbol{\varphi}_{\alpha,k}(t) = (2-\delta_{k,0}) \int_{-1}^{1} {\rm d}x\, T_k(x) \boldsymbol{\varphi}_{\alpha}(x,t), \tag{17}$$

$$\begin{aligned} \boldsymbol{\psi}_{\alpha'k',\alpha k}(t) = &\int_{-1}^{1} {\rm d}x'\, T_{k'}(x') \int_{-1}^{1} {\rm d}x\, T_k(x) \boldsymbol{\psi}_{\alpha',\alpha}(x',x,t) \\ &\times (2-\delta_{k',0})(2-\delta_{k,0}), \end{aligned} \tag{18}$$

and $\mathbf{\Pi}_{\alpha,k}(t)$'s and $\mathbf{\Xi}_{\alpha,k}(t)$'s, defined by Eqs. (19) and (20), respectively, are similarly computed with the help of Eq. (13),

$$\mathbf{\Pi}_{\alpha,k}(t) = \int_{-1}^{1} \mathrm{d}x\, T_k(x)\mathbf{\Lambda}_\alpha(x)\mathrm{e}^{-i\Omega x(t-t_0)}, \tag{19}$$

$$\mathbf{\Xi}_{\alpha,k}(t) = \int_{-1}^{1} \mathrm{d}x\, T_k(x)\bar{f}_\alpha(x)\mathbf{\Lambda}_\alpha(x)\mathrm{e}^{-i\Omega x(t-t_0)}. \tag{20}$$

The Bessel function decays to zero spectrally as n increases[12]

$$J_n(t) \sim \frac{1}{\sqrt{2\pi n}}\left(\frac{t\mathrm{e}}{2n}\right)^n \quad \text{as } n \to \infty, \quad \text{for a given } t, \tag{21}$$

therefore, the series in Eqs. (14) and (15) can be truncated after M terms, with M being around $1.5\Omega(t - t_0)$, if $\Omega(t - t_0)$ is large enough, and maybe much smaller than $1.5\Omega(t - t_0)$ in view of the requirement of accuracy in practical simulations, thus there is no need to worry about the convergence problem.

Besides, the correct initial condition should be provided in order to obtain physically meaningful result from Eqs. (14)–(16). Since at $t = t_0$ the total system is in the equilibrium state, all RSDM can be reformulated in the single-particle Green's function language[9] as follows:

$$\begin{aligned}
\mathbf{\Sigma}_\alpha^<(t_1 - t_2; x) &= \bar{f}_\alpha(x)\mathbf{\Lambda}_\alpha(x)\mathrm{e}^{-i\Omega x(t_1-t_2)},\\
\mathbf{\Sigma}_\alpha^>(t_1 - t_2; x) &= (1 - \bar{f}_\alpha(x))\mathbf{\Lambda}_\alpha(x)\mathrm{e}^{-i\Omega x(t_1-t_2)},\\
\boldsymbol{\sigma}(t_0) &= -i\mathbf{G}^<(t_0, t_0),\\
\boldsymbol{\varphi}_\alpha(x, t_0) &= i\int_{-\infty}^{t_0} \mathrm{d}\bar{t}\big[\mathbf{G}^<(t_0 - \bar{t})\mathbf{\Sigma}_\alpha^>(\bar{t} - t_0; x)\\
&\quad - \mathbf{G}^>(t_0 - \bar{t})\mathbf{\Sigma}_\alpha^<(\bar{t} - t_0; x)\big],
\end{aligned} \tag{22}$$

$$\begin{aligned}
&\boldsymbol{\psi}_{\alpha',\alpha}(x', x, t_0)\\
&= i\int_{-\infty}^{t_0} \mathrm{d}t_2 \int_{-\infty}^{t_2} \mathrm{d}t_1\big[\mathbf{\Sigma}_{\alpha'}^<(t_0, t_1; x')\mathbf{G}^a(t_1 - t_2)\mathbf{\Sigma}_\alpha^>(t_2 - t_0; x)\\
&\quad - \mathbf{\Sigma}_{\alpha'}^>(t_0 - t_1; x')\mathbf{G}^a(t_1 - t_2)\mathbf{\Sigma}_\alpha^<(t_2 - t_0; x)\big]\\
&\quad + i\int_{-\infty}^{t_0} \mathrm{d}t_2 \int_{-\infty}^{t_0} \mathrm{d}t_1\, \mathbf{\Sigma}_{\alpha'}^r(t_0 - t_1; x')\\
&\quad \times \big[\mathbf{G}^<(t_1 - t_2)\mathbf{\Sigma}_\alpha^>(t_2 - t_0; x)\\
&\quad - \mathbf{G}^>(t_1 - t_2)\mathbf{\Sigma}_\alpha^<(t_2 - t_0; x)\big].
\end{aligned} \tag{23}$$

Thereby, the most straightforward way to determine the initial condition is to make the best of the basic relations (17) and (18) at $t = t_0$, which has been elaborated on elsewhere.[13]

III. NUMERICAL CALCULATION OF A SIMPLE SYSTEM

To demonstrate the validity of this scheme, it is very instructive to test this new scheme on an one dimensional infinite nearest tight-binding chain illustrated in Fig. 1, of which, N, neighboring sites in the centre are chosen as the device part and the rest semi-infinite chain on the right/left side as the right/left electrode, respectively.

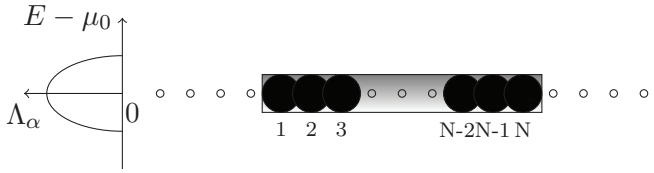

FIG. 1. An illustrative plot showing the 1-dimensional uniform infinite nearest tight-binding chain. The left panel shows the line-width function Λ_α.

It is assumed that the local orbitals $|n_j\rangle$'s on each site constitute a complete orthonormal basis set, and the electron is spinless. Since the hopping happens only between nearest neighboring sites, the total Hamiltonian for the whole infinite chain is

$$\mathbf{H}_\mathrm{T} = \sum_{j\in\mathbb{N}} \mu_0 a_j^\dagger a_j + v\big(a_j^\dagger a_{j-1} + a_{j-1}^\dagger a_j\big), \tag{24}$$

with v being the hopping term and μ_0 being the on-site energy, also the Fermi level of the whole infinite chain, can be written as an infinite-dimension tridiagonal real symmetric matrix. Due to this special structure, the line-width matrix $\mathbf{\Lambda}_\alpha$ is just a scalar function, and can be analytically calculated,[14]

$$\Lambda_\alpha(x) = |v|\sqrt{1 - x^2}, x \in [-1, 1], \tag{25}$$

and we have $\bar{\omega} = \mu_0$, $\Omega = 2|v|$.

In the left panel of Fig. 1, we plot Λ_α versus x. Indeed, it is not uniform. This exact $\Lambda_\alpha(x)$ is used in the calculation below. In our simulation, we assume that $v = 2.0$, $\mu_0 = 1.5$ and the desired length of propagation time is $t_{max} - t_0 = 15$, then the total number of $\boldsymbol{\varphi}_{\alpha,k}(t)$'s needed in this interval [0, 15] is 86, which results from the following criterion of truncation at $t = t_{max}$:

$$J_{k_{max}}(\Omega(t - t_0)) \geq 10^{-8}, \; J_{k_{max}+1}(\Omega(t - t_0)) < 10^{-8}. \tag{26}$$

After preparation of the initial condition, the bias voltage $\Delta_L(t) = 0.005\vartheta(t - t_0)$, $\Delta_R(t) = -0.005\vartheta(t - t_0)$, where $\vartheta(t)$ is the Heaviside step function, is symmetrically applied to left and right electrode, and then the explicit fourth-order Runge-Kutta algorithm is utilized to advance the HEOM (14)–(16) with the fixed time increment being 0.05.

In fact, the criterion of cutoff, 10^{-8}, which is quite moderate, can guarantee the reliability of the result with the time increment being 0.05.

In Fig. 2(a), two sets of transient currents are calculated from the criterion of truncation being 10^{-8} (solid line) and 10^{-12} (crosses), respectively, with temperature kept at *zero* and the time increment being still 0.05. The fact that the resulting transient current does not exhibit any discernible discrepancy even the criterion of cutoff is strengthened to 10^{-12}, as shown in Fig. 2(a), verifies that it is reliable to adopt the criterion of cutoff, 10^{-8}, which will be employed for the calculations thereinafter, and that the accuracy of this scheme can be immune to a wide range of criterion of truncation. The current overshoots initially and approaches the steady state value[15,16] with decreasing oscillation amplitude. Note that the oscillation persists beyond $t - t_0 = 10$, which can be seen in Fig. 3(a).

In Fig. 2(b), we plot the cubic root of the actual computational time on a single-core computer against various number

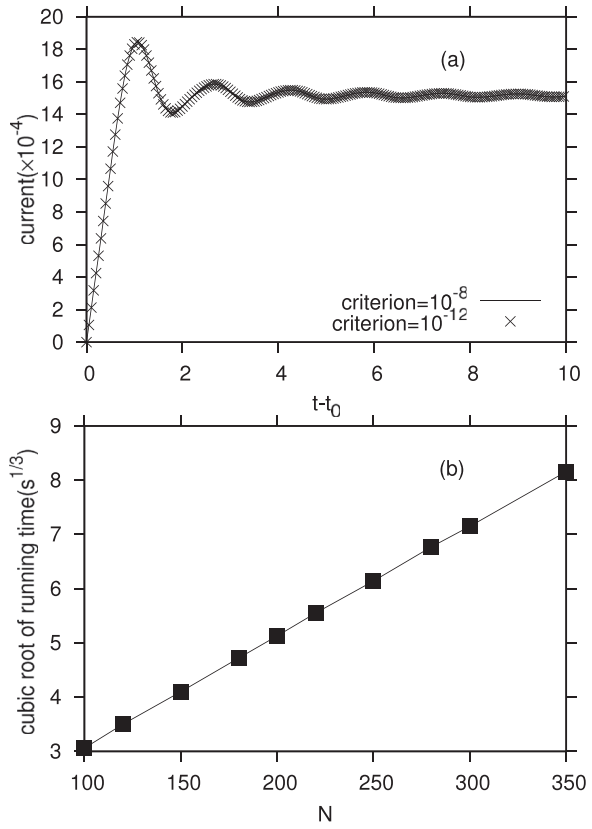

FIG. 2. (a) Currents of 3 sites in the device part, subjected to two different cutoffs; (b) the cubic root of the CPU time versus the number of sites N in the device part.

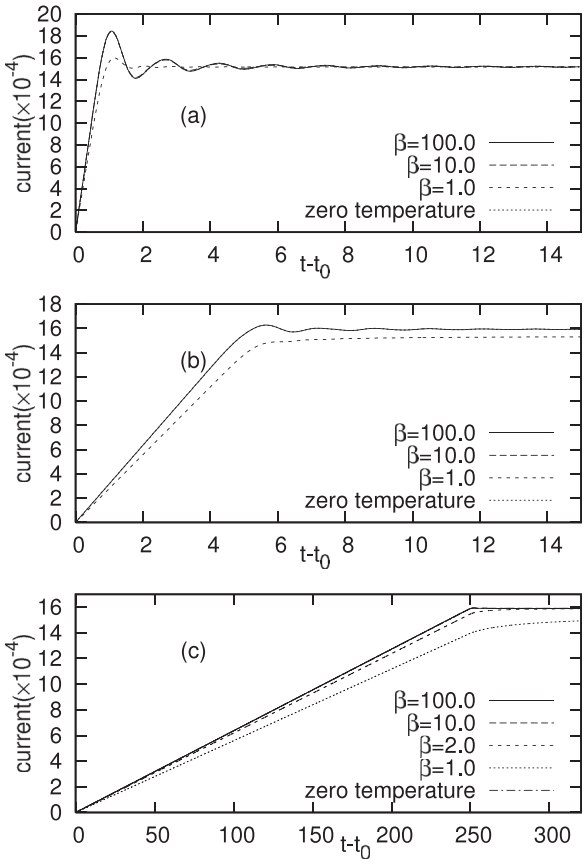

FIG. 3. (a) Currents of 3 sites at different temperature; (b) currents of 20 sites at different temperature; (c) currents of 1000 sites at different temperature.

of sites N in the device part with the same v, μ_0, $t_{max} - t_0$ and time increment. The perfect linearity of these data points confirms that the computational time scales *cubically* with the size of the device part, i.e., the central processing unit (CPU) time $\propto \mathcal{O}(N^3)$, and confirms the efficiency of the Chebyshev spectral decomposition scheme developed here.

To demonstrate that this Chebyshev spectral decomposition scheme is applicable to all temperatures, we simulate the transient current for different N's at a series of inverse temperatures $\beta = 1.0$, 10.0, 100.0, and ∞. We start with $N = 3$. The simulation results with $N = 3$ at different temperatures, subjected to the bias voltage $\Delta_L(t) = 0.005\vartheta(t - t_0)$, $\Delta_R(t) = -0.005\vartheta(t - t_0)$, are depicted in Fig. 3(a). The current at zero temperature in Fig. 3(a) coincides with the current with $\beta = 100.0$ or larger β, while the current with $\beta = 10.0$ can be barely distinguished from the former two. It is clear that for the system with $N = 3$, the higher the temperature is (or the smaller β is), the lower the overshooting is and the faster the current approaches its steady state value[15] as if due to stronger damping.

When 20 sites are in the device part with the same v, μ_0 and bias voltage, as is shown in Fig. 3(b), it is found that at high temperature, e.g., $\beta = 1.0$, the overshooting and oscillation of the transient current are completely suppressed. And even at lower temperatures, the amplitude of oscillation of transient current is much less than that in Fig. 3(a). It is noted that the current reaches its steady state value[15] at $t - t_0 \approx 5$. Moreover, the steady state current is clearly smaller at higher temperature for $N = 20$, which is far from obvious for $N = 3$. This is because the energy intervals of the device part for $N = 3$ are much greater than those for $N = 20$.

The results shown in Fig. 3(c) for $N = 1000$ with all other parameters kept the same as Figs. 3(a) and 3(b) are even more striking. The influence of the number of sites N in the device part and temperature becomes distinct. At all temperatures, the current increases linearly with time before reaching the steady state values. This is indicated in Fig. 3(b), but not clear in Fig. 3(a), i.e. , for $N = 3$. As N increases, this linearity becomes more and more evident, which has been observed and explained in another work of ours.[19] Note that for zero and lower temperatures at $t - t_0 = 250$, the steady state current is reached, and the time needed is five times as much as that for $N = 20$. This unexpected perfect linear increasing of the transient current with time,[19] gives further prominence to this exquisite approach. Also note that at high temperature, e.g., $\beta = 1.0$, the system approaches its steady state somewhat slower than that at lower temperature, while the results for $\beta = 10.0$ and $\beta = 100.0$ are indistinguishable from that of zero temperature, and that the dependence of the slope of the transient current on temperature shows up only at high temperature.

IV. DISCUSSION

To the best of our knowledge, there have been several attempts on the time-dependent quantum transport, which are

also based on TDDFT.[17,18] However, our method is quite distinct from the schemes in Refs. 17 and 18.

In Ref. 17, Baer *et al.* aim to extract the alternating current impedance and conductance of a molecular junction at *zero* temperature from *linear response* TDDFT calculation with adiabatic local density approximation. In their work,[17] the leads are modelled as jellium slabs, which disregards the atomic details of the leads, hence the absorbing potential, which amounts to the line-width matrix $\mathbf{\Lambda}_\alpha$ here, can only be specified with some empiric expressions and parameters. As a consequence, their results may differ from the calculations in the prevailing nonequilibrium Green's function (NEGF) method in the direct current case. On the contrary, in our method this line-width matrix $\mathbf{\Lambda}_\alpha$ takes full account of the atomic details of the leads in the same manner as the usual NEGF method combined with first-principles simulations, which is demonstrated in Sec. III. Moreover, our method can work at both zero and finite temperatures, and in both alternating and direct current cases.

In Ref. 18, Kurth *et al.* propose a practical propagation scheme of the time-dependent KS equation of an infinite dimension, and test it on some model systems. Both their method and ours start to apply the bias voltage from a well-defined thermodynamic equilibrium state, where the device part and the electrodes are connected, and go beyond the wide-band-limit approximation of the line-width matrix.[6] However, in their approach, it appears that only the retarded component of NEGF quantities has been employed, which differentiates their method from ours[9] fundamentally. It is believed that the lesser NEGF, or rather, the RSDM $\boldsymbol{\sigma}(t)$ in our case, will provide necessary information about the dynamic occupation number in the device part.

In both schemes of Refs. 17 and 18, the wave function plays an essential role, which leads to great difficulty, if not impossible, to make connection with the standard description of open system in quantum dissipation theory.[5] In contrast, in our method, we adhere to the standpoint of the latter throughout and hence circumvent this obstacle caused by wave function approach. Besides, regarding the numerical scheme of advancing their respective EOM of wave function, the absorbing boundary conditions or transparent boundary conditions have been imposed, which, however, is irrelevant to our method. While in common with the Baer's scheme, we need the electrostatic and the exchange-correlation potential of the device part to update $\mathbf{H}_\mathrm{C}$, in our method, the electrostatic potential is obtained as the solution of the Poisson equation with the boundary conditions that arise naturally from requiring the continuity of the electrostatic potential at the interfaces between the electrodes and the device part.[1] Moreover, in both schemes, the transient current through the molecular junction is calculated from the surface integration of the current density, while in our method, the current density is unnecessary since the current is simply the trace of some matrices, as shown in Eq. (12).

In our method, the explicit fourth-order Runge-Kutta algorithm is utilized, which allows longer time increment at the same level of accuracy compared to Crank-Nicholson algorithm in Kurth's method. Moreover, in several plots of time evolution of the current in Ref. 18, strong oscillations of the transient current are observed just after turning on the bias voltage, which, however, do not show up in our simulations with similar set up in Sec. III.

V. CONCLUSION

The Chebyshev spectral decomposition algorithm is proposed and developed to integrate the single-particle Liouville-von Neumann equation, which leads to a new set of HEOM that are solved for a chain of atoms or quantum dots (QDs) described by the tight-binding model. The computational time of the new algorithm scales *cubically* with the system size, i.e. , $\mathcal{O}(N^3)$, thus, is highly efficient and applied to simulate the transient current through a chain of atoms or QDs up to 1000 orbitals, while the conventional methods are normally applicable only to the systems with a few orbitals. More importantly, the Chebyshev spectral decomposition algorithm covers both zero and high temperatures, while no other existing methods in quantum dissipation theory are capable of. Our simulation shows convincingly that temperature dampens the overshooting and oscillation of the transient currents and lowers the magnitude of the steady state current. Surprisingly, the increasing size of the system has the similar effects as temperature, such as dampening the overshooting and oscillation. Our calculation confirms that the transient current increases linearly with time as N is large enough, a novel phenomena found in another work.[19] Although it is implemented at the tight-binding level, the Chebyshev spectral decomposition scheme can be combined with first-principles methods, e.g., TDDFT. The memory (non-Markovian) effect due to the electrodes is fully accounted for, as the exact line-width matrix is employed. It would also be interesting to extend the method to other phenomena of open systems beyond quantum transport.

ACKNOWLEDGMENTS

Support from the Hong Kong Research Grant Council (Contract Nos. HKU7009/09P, 7008/11P, and HKUST 9/CRF/08), and the University Grant Council (Contract No. AoE/P-04-08) is gratefully acknowledged. The first author greatly appreciates the discussion with Dr. Lijun Jiang.

[1] X. Zheng, F. Wang, C. Y. Yam, Y. Mo, and G. H. Chen, Phys. Rev. B **75**, 195127 (2007).
[2] H. Tal-Ezer and R. Kosloff, J. Chem. Phys. **81**, 3967 (1984); R. Kosloff, *ibid.* **92**, 2087 (1988); Annu. Rev. Phys. Chem. **45**, 145 (1994); R. Q. Chen and H. Guo, J. Chem. Phys. **105**, 3569 (1996).
[3] W. Kohn and L. J. Sham, Phys. Rev. **140**, A1133 (1965).
[4] E. Runge and E. K. U. Gross, Phys. Rev. Lett. **52**, 997 (1984).
[5] J. S. Jin, X. Zheng, and Y. J. Yan, J. Chem. Phys. **128**, 234703 (2008).
[6] A.-P. Jauho, N. S. Wingreen, and Y. Meir, Phys. Rev. B **50**, 5528 (1994).
[7] Y. Tanimura, Phys. Rev. A **41**, 6676 (1990).
[8] J. S. Shao, J. Chem. Phys. **120**, 5053 (2004).
[9] X. Zheng, G. H. Chen, Y. Mo, S. K. Koo, H. Tian, C. Y. Yam, and Y. J. Yan, J. Chem. Phys. **133**, 114101 (2010), and references therein.
[10] A. Croy and U. Saalmann, Phys. Rev. B **80**, 245311 (2009).
[11] T. N. L. Patterson, Numer. Math. **27**, 41–52 (1976).
[12] M. Abramowitz and I. A. Stegun, *Handbook of Mathematical Functions* (Dover, New York, 1965).
[13] H. Tian, Ph.D. dissertation (University of Hong Kong, 2012).

[14]I. Appelbaum, T. Wang, J. D. Joannopoulos, and V. Narayanamurti, Phys. Rev. B **69**, 165301 (2004).
[15]R. Landauer, IBM J. Res. Dev. **32**, 306 (1988), and references therein; M. Büttiker, Phys. Rev. Lett. **57**, 1761 (1986).
[16]C. Y. Yam, X. Zheng, G. H. Chen, Y. Wang, T. Frauenheim, and T. A. Niehaus, Phys. Rev. B **83**, 245448 (2011).
[17]R. Baer, T. Seideman, S. Ilani, and D. Neuhauser, J. Chem. Phys. **120**, 3387 (2004).
[18]S. Kurth, G. Stefanucci, C.-O. Almbladh, A. Rubio, and E. K. U. Gross, Phys. Rev. B **72**, 035308 (2005).
[19]S. G. Chen, H. Xie, Y. Zhang, X. D. Cui, and G. H. Chen, "Quantum transport through an array of quantum dots," Nanoscale (to be published).